frontiers in Marine Science

ORIGINAL RESEARCH
published: 10 July 2020
doi: 10.3389/fmars.2020.00558

Regional Movements of Reef Manta Rays (*Mobula alfredi*) in Seychelles Waters

Lauren R. Peel[1,2,3,4], Guy M. W. Stevens[3], Ryan Daly[4,5,6], Clare A. Keating Daly[4], Shaun P. Collin[1,7], Josep Nogués[8] and Mark G. Meekan[2]*

[1] School of Biological Sciences, Oceans Institute and Oceans Graduate School, The University of Western Australia, Crawley, WA, Australia, [2] The Australian Institute of Marine Science, Crawley, WA, Australia, [3] The Manta Trust, Corscombe, United Kingdom, [4] Save Our Seas Foundation – D'Arros Research Centre, Geneva, Switzerland, [5] South African Institute for Aquatic Biodiversity, Grahamstown, South Africa, [6] Oceanographic Research Institute, Durban, South Africa, [7] School of Life Sciences, College of Science, Health and Engineering, La Trobe University, Bundoora, VIC, Australia, [8] Island Conservation Society, Pointe Larue, Seychelles

The decline in numbers of reef manta rays (*Mobula alfredi*) throughout their range has highlighted the need for improved information on their spatial ecology in order to design effective conservation strategies for vulnerable populations. To understand their patterns of movement in Seychelles, we used three techniques—archival pop-up satellite tags, acoustic tags, and photo-identification—and focussed on the aggregation at D'Arros Island and St. Joseph Atoll within the Amirantes Group. *M. alfredi* were photographed within six of the seven Island Groups of Seychelles, with 64% of individuals being resighted at least once between July 2006 and December 2019 over timeframes of 1–3,462 days (9.5 years; median = 1,018 days). Only three individuals from D'Arros Island were resighted at a second aggregation site located more than 200 km away at St. François Atoll during photo-identification surveys. Satellite-tracked *M. alfredi* (n = 5 tracks; maximum 180 days) remained within the boundary of the Seychelles Exclusive Economic Zone, where they spent the majority of their time (87%) in the upper 50 m of the water column in close proximity to the Amirantes Bank. The inclusion of acoustic tagging data in the models of estimated satellite-track paths significantly reduced the errors associated with the geolocation positions derived from archived light level data. The insights gained into the patterns of horizontal and vertical movements of *M. alfredi* using this multi-technique approach highlight the significance of D'Arros Island and St. Joseph Atoll, and the wider Amirantes Group, to *M. alfredi* in Seychelles, and will benefit future conservation efforts for this species within Seychelles and the broader Western Indian Ocean.

Keywords: spatial ecology, acoustic telemetry, satellite telemetry, geolocation, Western Indian Ocean, conservation

OPEN ACCESS

Edited by:
Lars Bejder,
University of Hawai'i at Mānoa,
United States

Reviewed by:
Nuno Queiroz,
University of Porto, Portugal
Philip D. Doherty,
University of Exeter, United Kingdom

****Correspondence:***
Lauren R. Peel
laurenrpeel@gmail.com

Specialty section:
This article was submitted to Marine Megafauna, a section of the journal Frontiers in Marine Science

Received: *07 February 2020*
Accepted: *17 June 2020*
Published: *10 July 2020*

Citation:
Peel LR, Stevens GMW, Daly R, Keating Daly CA, Collin SP, Nogués J and Meekan MG (2020) Regional Movements of Reef Manta Rays (Mobula alfredi) in Seychelles Waters. Front. Mar. Sci. 7:558. doi: 10.3389/fmars.2020.00558

INTRODUCTION

Reef manta rays (*Mobula alfredi*; Marshall et al., 2009; White et al., 2017) are large, zooplanktivorous elasmobranchs with a circumtropical distribution (Couturier et al., 2012; Stewart et al., 2018). Aggregations of these mobulid rays (Family Mobulidae; Notarbartolo di Sciara, 1987; Couturier et al., 2012; White et al., 2017) occur at numerous locations around the world, however, they are

being increasingly exploited for their gill plates for use in the Asian medicinal trade (White et al., 2006; O'Malley et al., 2017). This fishing pressure, coupled with the impacts of other anthropogenic threats, including boat strike, accidental entanglement, and by-catch, has resulted in global declines of *M. alfredi* populations (Couturier et al., 2012; Croll et al., 2016; Stewart et al., 2018). In the last decade, positive conservation measures for *M. alfredi* have been taken at the international level (Croll et al., 2016; Marshall et al., 2018). However, at local (i.e., regional and national) scales, where intensive fishing practices can cause rapid and persistent declines in populations (Dewar, 2002; Rohner et al., 2017; Marshall et al., 2018), management strategies are less defined and can be difficult to establish. Local management is further complicated by the ability of *M. alfredi* to travel large distances away from the aggregation sites at which they are commonly sighted (50–1,150 km; Couturier et al., 2011; Deakos et al., 2011; Jaine et al., 2014; Armstrong et al., 2019). Such movements highlight the difficulty associated with quantifying the magnitude and impact of anthropogenic pressures on *M. alfredi* populations throughout their range. An understanding of the patterns of movement and habitat use of *M. alfredi* not only at aggregation areas, but also away from these sites, is therefore critical to the design of effective conservation measures aimed at protecting their populations from unsustainable exploitation at local scales.

Satellite tracking represents an effective means to monitor the movement patterns of megafauna (Hays et al., 2016; Sequeira et al., 2018) and is providing researchers insights into both the large (100s to 1000s of km) and fine (0.1s to 1s of km) scale movement patterns of *M. alfredi* (Braun et al., 2014, 2015; Jaine et al., 2014; Kessel et al., 2017; Andrzejaczek et al., 2020). Datasets retrieved from archival pop-up satellite tags can be used to visualize the horizontal extent of movement of individuals throughout their home range, and can also reveal the drivers of horizontal and vertical movements through the water column (Canese et al., 2011; Jaine et al., 2014; Kessel et al., 2017; Andrzejaczek et al., 2018; Lassauce et al., 2020). In contrast to satellite tags that communicate solely with satellites to report the locations tagged individuals (e.g., SPOT tags), pop-up archival tags are also programmed to log light, temperature, and depth data for a predetermined period of time. Upon release from the individual, archived data are transmitted from the tag in segments via satellite, or downloaded in full when the tag is retrieved. Geolocation processes are then used to estimate the most-likely track path of tagged individuals based on available light, sea surface temperature, and bathymetric data (Teo et al., 2004). By staggering satellite tag deployments over field expeditions throughout the year, it becomes possible to consider movement patterns on seasonal and annual scales (Weng et al., 2007; Braun et al., 2018b). The prohibitive cost of satellite tags, however, limits deployment numbers and is the primary barrier to obtaining representative sample sizes for many species, including manta rays (Hays et al., 2016). Furthermore, the errors surrounding location estimates that are generated using light data reduces the accuracy of horizontal tracks provided by pop-up tags, particularly in the tropics (Teo et al., 2004; Braun et al., 2014, 2018a), where the majority of *M. alfredi* populations occur (Kashiwagi et al., 2011; Couturier et al., 2012).

Acoustic telemetry offers an alternative to archival pop-up satellite tagging as a means of describing movement patterns of *M. alfredi* (Clark, 2010; Braun et al., 2015; Couturier et al., 2018; Setyawan et al., 2018; Andrzejaczek et al., 2020). Acoustic tags transmit a uniquely coded signal that is passively detected whenever the tagged individual moves within the detection radius of receivers deployed at the study site (Heupel et al., 2006). Although many more animals can be monitored using acoustic tags due to their lower cost (relative to satellite tags), acoustic tracking is restricted to the spatial extent of the receiver array that is deployed to detect tagged individuals (Stewart et al., 2018). Additionally, receivers must be recovered and downloaded to obtain detection data (Heupel et al., 2006).

In contrast to the cost and logistics involved with satellite and acoustic tagging, photo-identification offers a simple means to examine site-fidelity and movement patterns of *M. alfredi* (Marshall and Pierce, 2012). Photographs of the unique and permanent ventral markings on individual *M. alfredi* can be used to examine levels of site fidelity and residency exhibited by cohorts of a population, and to assess the frequency at which individuals travel between aggregation sites (Kitchen-Wheeler, 2010; Deakos et al., 2011; Marshall et al., 2011; Marshall and Pierce, 2012). This technique is, however, usually biased to areas where *M. alfredi* are already known to aggregate, and information on the fine-scale (hours to days) movements of individuals between locations is often absent (Deakos et al., 2011). Additionally, it can be logistically difficult to gain access to and continuously survey aggregation sites, particularly in remote locations. These challenges can result in seasonally biased datasets that may not be completely representative of the annual movement patterns of the population.

Some of the shortcomings of satellite and acoustic tagging, and photo-identification techniques, may be overcome by combining these approaches (Meyer et al., 2010; Kneebone et al., 2014; Vianna et al., 2014; Braun et al., 2015). Detections of acoustic tags within receiver arrays, individually or combined with sighting records of tagged individuals at aggregation sites, can be used to reduce the uncertainty surrounding location estimates derived from geolocation analyses (Werry et al., 2014; Cochran et al., 2019). This combined approach improves the accuracy of individual tracks provided by archival pop-up tags. In turn, tracking data can provide a better picture of both large-scale movement and home range of individuals, allowing researchers to determine the extent to which acoustic tagging and photo-identification techniques are likely to capture residency and movement patterns over a range of spatial scales (Kneebone et al., 2014; Vianna et al., 2014). Furthermore, the variable periods of time over which these techniques are typically applied [3–6 months for satellite tags (Jaine et al., 2014; Braun et al., 2015), up to 10 years for internally implanted acoustic tags (Kessel et al., 2017), and potentially ongoing for photo-identification (Couturier et al., 2014)] provide insight into the conservation needs of this species over a range of temporal scales. Collectively, these spatiotemporal data can be used to develop scientifically informed management and conservation strategies for the species

[e.g., Marine Protected Areas (MPAs); Germanov and Marshall, 2014; Peel et al., 2019b; Dwyer et al., 2020], and guide future research and monitoring efforts at both local scales (i.e., at aggregation sites and within populations), and more broadly throughout the range of *M. alfredi*.

Here, we combined satellite and acoustic tracking and photo-identification techniques to examine the movement ecology of *M. alfredi* in the remote reef systems of Seychelles, with a focus on the aggregation at D'Arros Island within the Amirantes Group. These data were used to determine the home range size and regional movement patterns of individuals, and to assess potential drivers of their patterns of horizontal and vertical movement. Data were also used to examine the efficacy of MPAs to conserve *M. alfredi* in Seychelles, and to inform future research efforts for the species throughout the country and across the wider Western Indian Ocean region.

MATERIALS AND METHODS

Study Site

The Republic of Seychelles is a nation comprising 115 islands in the tropical Western Indian Ocean that are divided into two main groups; the more populous and granitic Inner Islands, and the relatively remote, coralline Outer Islands. The Outer Islands are divided into six smaller groups—Aldabra, Alphonse, Amirantes, Farquhar, Northern Corallines, and Southern Corallines—based on geographic location (**Figure 1**).

Reliable aggregations of *M. alfredi* are currently known to occur within the Amirantes and Alphonse Groups. These two Island Groups are often considered collectively (i.e., as the Amirantes Group), however, are discussed separately in this study. The 24 islands and islets of the Amirantes Group, with the exception of Desroches Atoll, are located across the Amirantes Bank (30 × 160 km); a predominantly shallow (<40 m average depth) shelf that reaches maximum depths of 70 m in the center, before waters descend rapidly to depths of over 1,000 m off the Bank ridge (**Figure 1**; Stoddart et al., 1979). D'Arros Island and St. Joseph Atoll are situated centrally along the eastern ridge of the Bank and host a year-round aggregation of *M. alfredi* (Peel, 2019; Peel et al., 2019b). Previous studies have used acoustic telemetry to study local movement and residency patterns of elasmobranchs throughout the Amirantes Islands and, as a result, a network of passive acoustic receivers exists throughout the region (**Figure 1**; Lea et al., 2016; Peel et al., 2019b).

Alphonse Atoll and the St. François Atoll comprise the Alphonse Group, and are located 80 km to the south of the Amirantes Bank (**Figure 1**; Hamylton et al., 2012). The extensive reef flats, two islands, and three-chambered lagoon of the St. François Atoll span a collective area of 53 km^2. Sightings of *M. alfredi* feeding along the edges of the reef flats and within the northern-most lagoon are common at this location, particularly during the north-west monsoon when the area is accessible to human visitors (November to March; L. Peel, unpublished data).

Photo-Identification

Identification photographs of individual *M. alfredi* were collected across three spatiotemporal scales in Seychelles to monitor

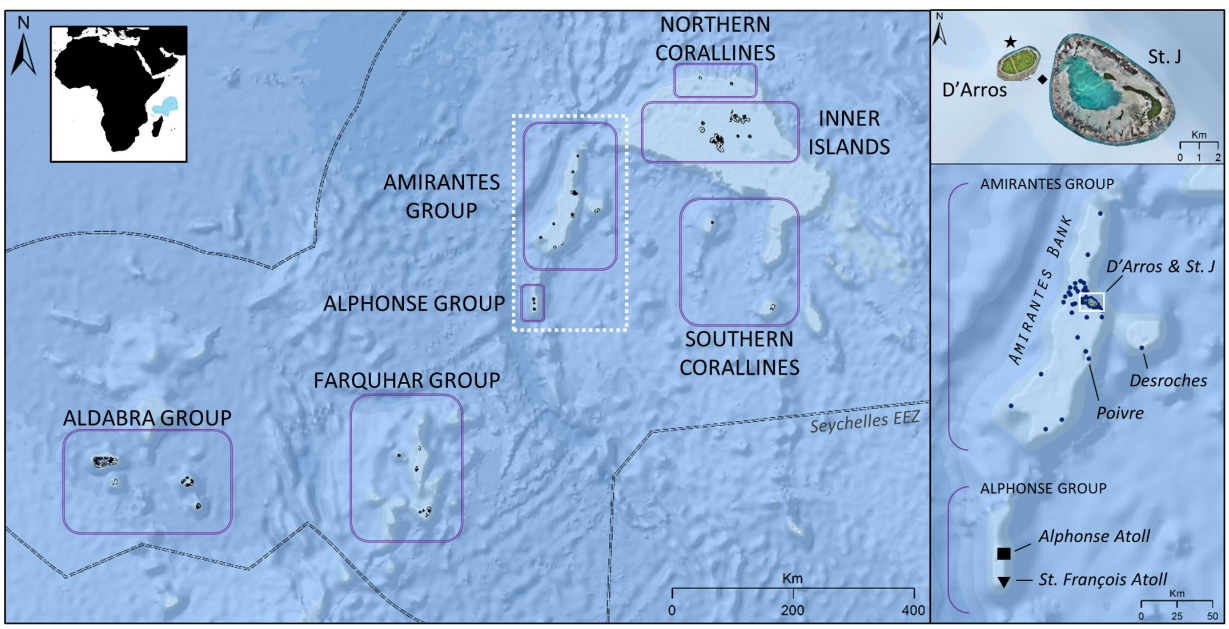

FIGURE 1 | Location of the seven Island Groups of Seychelles [Exclusive Economic Zone (EEZ) of country indicated in blue in inset map]. Reef manta rays (*Mobula alfredi*) are frequently sighted near D'Arros Island and St. Joseph Atoll (St. J) within the Amirantes Group, and at St. François Atoll within the Alphonse Group. Seventy acoustic receivers (•) are deployed within the Amirantes Group. Alphonse Atoll located at "■"; St. François Atoll located at "▼"; D'Arros Island manta cleaning station located at "★"; St. Joseph channel (depth 60 m) located at "♦". Satellite imagery © Save Our Seas Foundation.

the movement patterns of this population (Marshall et al., 2009; Peel, 2019). A manta ray "sighting" was defined as a confirmed photo-identification of an individual at a specific site on a specific day. Broadly, sightings of *M. alfredi* were recorded opportunistically throughout Seychelles by the authors, collaborators, and members of the public between July 2006 and December 2019. More specifically, sightings were recorded during three dedicated manta surveys at D'Arros Island and St. Joseph Atoll (November 2013, November 2016, and November 2017), and one dedicated manta survey at Alphonse Atoll and St. François Atoll (2–9 December 2017). Lastly, a remote camera system was deployed at a manta ray cleaning station to the north of D'Arros Island between 29 September 2017 and 27 November 2017 in order to continuously monitor visits of *M. alfredi* to this site. The remote camera system consisted of a single GoPro Hero4 (GoPro; CA, United States) with a Blink time-lapse controller, which was attached by a USB splitter cable to two Voltaic LiPo 44 Wh batteries with an "always-on" feature. The camera and batteries were housed within a 17 × 29 cm PVC cylinder, which was sealed with a 2.3 cm thick acrylic lid with an o-ring and metal latches. The time lapse for the GoPro was set to take an image every 10 s, allowing for deployment periods of approximately 48 h prior to battery depletion. Constant monitoring of the cleaning station was made possible using two MantaCam systems, whereby one camera was deployed as the other was retrieved.

All recorded sightings of *M. alfredi* included an identification image of the unique pigmentation pattern on the ventral surface of each individual and details of the time and location of the encounter (Marshall et al., 2011; Marshall and Pierce, 2012). Collected images were stored in an online database, and identifications were completed by manually comparing each photograph to a reference library of previously sighted individuals. The presence (male) or absence (female) of claspers was used to determine the sex of each individual (Marshall et al., 2009), and the extent of calcification of the claspers used as a proxy for the maturity status of males (Marshall and Bennett, 2010). Mating scars and pregnancy bulges were used as indicators of sexual maturity in females, when present (Marshall and Bennett, 2010). The size (disc width) of all encountered individuals was visually estimated to the nearest 0.1 m, and these estimates were verified using a diver-operated stereo-video camera system wherever possible (Letessier et al., 2015). The stereo-video system consisted of two GoPro Hero4 Silver edition cameras mounted 70 cm apart on a base bar inwardly converged at 6°, and individual disc widths were measured using the program EventMeasure (SeaGIS). Individual sizes were also considered when estimating maturity status. Individuals were subsequently categorized into three life history stages: juvenile (any individual, ≤2.4 m), sub-adult (male, 2.5–2.8 m; female, 2.5–3.1 m), or adult (male, ≥2.9 m; female, ≥3.2 m; Stevens, 2016). Re-sightings of individuals, defined as sightings of individuals recorded after the first sighting of that individual, were used to monitor the frequency at which *M. alfredi* moved between locations over time.

Satellite Telemetry

Tag Deployment

Eight archival pop-up satellite tags (miniPATs; Wildlife Computers; Redmond, WA, United States) with titanium anchors and 10 cm stainless steel tethers were deployed between November 2016 and March 2019 in Seychelles (**Table 1**). Tags were externally deployed on the posterior dorsal surface of free-swimming *M. alfredi* using a modified Hawaiian sling either by SCUBA divers at a manta ray cleaning station, or by free divers at the surface. Two tags were deployed on two mature females at D'Arros Island in November 2016 (disc widths 3.0 and 3.6 m). An additional mature female was tagged at D'Arros Island in November 2017 (disc width 3.4 m). This latter individual was carrying an external acoustic tag that was deployed in a previous study (V16TP-5H; Vemco; Nova Scotia, Canada; see Peel et al., 2019b). The remaining five tags were deployed on males; two mature males at D'Arros Island in November 2017, one sub-adult male at St. François Atoll in December 2017, and two additional mature males at D'Arros Island in March 2019 (disc widths 3.0, 3.0, 2.5, 3.6, and 3.0 m, respectively).

Tags deployed in 2016 and 2017 were programmed to release after 180 days, whereas tags deployed in 2019 were programmed to release after 90 days. All tags were programmed to archive light level, depth, and water temperature data every 5 s. Archived data were summarized every 6 h for transmission, with the upper limits of storage bins for time-at-depth dataset to 0, 1, 5, 10, 20, 35, 50, 65, 80, 100, 150, 300, 2000 m, and for time-at-temperature data to 3, 6, 9, 12, 15, 18, 21, 24, 27, 30, 33, 45°C. In the event of an early release, tags were programmed to transmit summarized data via the Argos satellite system after a period of 36 h (tags deployed in 2016), or 24 h (tags deployed in 2017 and 2019), at a constant depth (±1.5 m) until battery failure or tag retrieval.

Geolocation

Data retrieved via satellite from all miniPATs were decoded using Wildlife Computers' online portal-based software and quality checked prior to analysis. Three tags were noted to have drifted at the surface for a period longer than scheduled (i.e., >36 or 24 h) before transmitting data. Retrieved depth and temperature data were subsequently examined to confirm accurate tag release times for all tags. The end time of each track was deemed to be the time before which all subsequent depth records from the tag were <0.5 m. No GPS locations were assigned to the final estimated track end times for each tag because we could not quantify the true distance between the first reported pop-up location of the tag and the real release location. Light level data were then examined to ensure that only single time estimates of dawn and dusk were recorded per day for each track. Where duplicate estimates were presented for either event, the later time was removed from the dataset. Lastly, for individual M4, an additional location point from a re-sighting event recorded through photo-identification was included in the final dataset.

Geolocation processing was completed using a hidden Markov model (HMM, WC-GPE3, Wildlife Computers) that considered archived light level, temperature, and depth data alongside sea

TABLE 1 | Summary of satellite tag deployments on reef manta rays (*Mobula alfredi*) in Seychelles including length of track (duration in days) and percentage of archived data decoded via satellite.

Manta ID	PTT	Sex	Disc width (m)	Tag date	Deployment location		Track end date	Duration (days)	Decoded (%)	Days with light data (%)
					Lat (°S)	Long (°E)				
M1	166070	F	3.0	27 Nov 2016	−5.409	53.299	07 Mar 2017	100	88	100
M2	166071	F	3.6	28 Nov 2016	−5.409	53.299	19 Jan 2017	52	88	100
M3‡	41817	M	3.0	17 Nov 2017	−5.409	53.301	06 Apr 2018	140	68	9
M4	41818	M	3.0	17 Nov 2017	−5.409	53.301	16 May 2018	180	44	29
M5*	41819	F	3.4	22 Nov 2017	−5.441	53.315	05 Apr 2018	134	84	100
M6	44321	M	2.5	03 Dec 2017	−7.066	52.757	–	DNR	–	–
M7	49000	M	3.6	04 Mar 2019	−5.425	53.299	–	DNR	–	–
M8	49002	M	3.0	04 Mar 2019	−5.412	53.296	02 Jun 2019	90	72	96

Asterisk indicates an individual that was carrying an active acoustic tag at the time of satellite tagging. ‡ Indicates the tag that transmitted insufficient and unreliable data for analysis. F, female. M, male. DNR, did not respond.

surface temperature (NOAA OI SST V2 High Resolution[1]) and bathymetric constraints (ETOPO1-Bedrock). After collating the available data, the HMM calculated a posterior probability distribution that estimated the most likely position of each individual at every time point of the track (Skomal et al., 2017). The diffusion parameter (i.e., most-probable speed) for *M. alfredi* was set to 1.2 m s^{-1} for all individuals, based on maximum speeds reported for this species moving through a coastal acoustic receiver array in the eastern Indian Ocean (F. McGregor, pers. comm.). Track paths were only estimated for tags that had light level data for >10% of the tracking days ($n = 5$) to avoid excessive interpolation occurring in tracks.

Inclusion of acoustic telemetry data in geolocation analysis

A total of 481 acoustic detections were retrieved throughout the Amirantes acoustic receiver array from the acoustic tag concurrently deployed alongside the miniPAT on individual M5. A second HMM was constructed for this individual that included these acoustic data as known positions (error radius 165 ± 33 m; Lea et al., 2016), alongside the positions estimated from the archived dataset. The same quality checks and model parameters were used to construct this secondary HMM, and this facilitated a comparison between the metrics of a geolocated track considering light level data alone (GPE3), to one that was based upon light level data and a substantial amount of additional location information (GPE3/A).

Horizontal Movement

Patterns of horizontal movement were visualized in ArcGIS 10.3 (ESRI, Redlands, CA, United States) over the ESRI World Ocean Basemap and analyzed in ArcMap and R (version 3.4.1; R Core Team, 2017). First, the most-probable track for each individual was mapped in ArcMap to visualize the extent of movement of each individual away from the tagging location and throughout the waters of Seychelles. A subset of the 50% error radii associated with the geolocated positions for each individual were then averaged as a measure of geolocation accuracy relative to the acoustic detection data retrieved for individual M5. As these radii were initially presented as an ellipse around each geolocated position, the perimeter length of each ellipse was used as a pseudo-circumference value to estimate the approximate radius of error.

Home range estimates for tagged individuals were calculated using normalized utilization distributions (NUDs), as described by Doherty et al. (2017). Briefly, the full set of 12-h likelihood surfaces that were calculated through the HMM analysis of geolocated data for each tag were compiled and averaged to examine where each individual was most likely to have occurred throughout the entirety of its track. Core home range areas were defined by NUD probabilities of ≤50%, whereas the extent of an individuals' home range was defined by the area encompassing NUD probabilities of ≤95%. The areas encompassing NUD probabilities ≤ 75% were also calculated to better visualize the patterns of movement and home range of tagged individuals. Although not accounting for the time-steps between recorded positions—as is possible using analytical methods such as Brownian-Bridge movement models (Horne et al., 2007), which failed to converge for these data—NUDs allowed for the large error radii (up to 137.9 km) associated with position estimates to be included. Furthermore, the use of NUDs allowed for the variation in error radii across likelihood surfaces to be considered in all home range analyses; contrasting with more traditional methods of home range estimation, such as standard kernel utilization distributions, which rely on a single estimate of error (e.g., Calenge, 2006). Collectively, this allowed for the NUDs to provide a more accurate view of the potential home range size of *M. alfredi* in Seychelles.

Vertical Movement

Transmitted depth and temperature data were analyzed using the package *RchivalTag* (Bauer, 2018) in R. *M. alfredi* are thought to vary foraging strategies, and thus patterns of vertical habitat use throughout the diel cycle, in response to shifting prey fields (Braun et al., 2014; Peel et al., 2019a). For this reason, two-sample Kolmogorov–Smirnov (K-S) tests were used to investigate whether the depth distribution for *M. alfredi* differed between the day (06:00–18:00) and the night (18:00–06:00). Additionally, two-sided Wilcoxon rank sum tests were used to determine if *M. alfredi* dived to different mean depths during the day and

[1]https://psl.noaa.gov/

the night. Both of these analyses were applied to data for each individual, as well as to a pooled dataset of all individuals. General linear models (GLMs) were then used to determine whether average nightly dive depth varied per tagged individual with respect to the lunar cycle. Moon illumination data for this latter investigation were accessed from the "Suncalc.net" project[2] using the package *suncalc* (Agafonkin and Thieurmel, 2018) in R, and arcsine transformed prior to analysis (Zar, 1996). When GLM residuals were found to be non-normally distributed through a Shapiro–Wilk test for normality ($p < 0.05$), a Spearman's rank correlation was used to investigate this relationship. To examine the generality of this relationship across all tagged individuals, a generalized linear mixed model (GLMM) with a Gamma error distribution and incorporating manta ID as a random effect was applied to the pooled dataset using the package *lme4* (Bates et al., 2015). This model was compared to the null (intercept-only) model (average dive depth $\sim 1 +$ manta ID) using an information-theoretic approach, and the top model was selected based on Akaike's information criterion corrected (AICc) for sample size and AICc weights [wAICc; ranging from 0 (no support) to 1 (full support)] (Thums et al., 2018). When the difference in AICc values (ΔAICc) between candidate models was <2 AICc units, the models were considered to be equally ranked and the most parsimonious model (i.e., containing the lowest number of explanatory variables) was selected (Ferreira et al., 2017). Lastly, transmitted depth data were examined relative to the average depth of the Amirantes Bank (∼40 m) and the depth of the St. Joseph Channel between D'Arros Island and St. Joseph Atoll (∼60 m; see **Figure 1**). This was done by quantifying the proportion of total depth records that were reported above each of these depths for all tagged individuals.

For all analyses, values of the standard deviation are presented with means unless otherwise stated.

RESULTS

Photo-Identification

Photo-identification was used successfully in Seychelles at three spatiotemporal scales to identify 252 individual *M. alfredi* throughout the Republic between July 2006 and December 2019. A total of 1,609 confirmed sightings were reported across the Aldabra (0.3%), Alphonse (7.8%), Amirantes (90.3%), Farquhar (0.3%), Inner (1.1%), and Northern Coralline (0.2%) Groups. No confirmed sightings of *M. alfredi* were recorded at the Southern Coralline Islands. A total of 160 (63.5%) of these individuals were resighted on at least one occasion (max = 60; **Figure 2**), over time frames of 1–3,462 days (9.5 years; median = 1,018 days), with the vast majority sighted within the same Island Group where they were first sighted (99.8% of all recorded re-sightings). The elapsed time between subsequent re-sightings ranged from 0 to 2,808 days (mean = 119 days, median = 7 days). At D'Arros Island and St. Joseph Atoll, 161 individual *M. alfredi* were identified across 1,429 sightings. A total of 119 (73.9%) of these individuals were resighted on at least one occasion at D'Arros Island and St. Joseph Atoll, with 17 (10.6%) also being resighted elsewhere in the Amirantes Group at either Desroches Atoll ($n = 1$) or Poivre Atoll ($n = 16$; see **Figure 1**).

Only three individuals moved between Island Groups on single occasions (**Supplementary Table S1**). All of these movements were from D'Arros Island (Amirantes Group) to St. François Atoll (Alphonse Group), and the time between subsequent re-sightings at these locations ranged from 14 to 1,624 days (∼4.5 years). The shortest of these >200 km journeys was 14 days, during which time the resighted individual would have traveled at a minimum straight-line speed of 13.9 km d^{-1} (0.16 m s^{-1}).

The eight *M. alfredi* satellite-tagged in this study had varying sighting histories prior to the deployment of the miniPATs (**Table 2**), but all had only been recorded within a single Island Group. Only two individuals were resighted through photo-identification after the release of their tags as of December 2019. Tagged individual M4 was resighted in the Amirantes Group at Poivre Atoll on 15 November 2018 (see **Figure 1**), after being tagged 40 km away at D'Arros Island 364 days earlier. Individual M6, whose tag failed to respond, was also resighted. This individual was observed feeding in a large aggregation event at St. François Atoll on 19 December 2018, 382 days after it was tagged in the same location.

Satellite Telemetry

Six of the eight miniPATs deployed on *M. alfredi* in Seychelles successfully transmitted data, all of which were deployed at D'Arros Island (**Table 3**). The single tag deployed at St. François Atoll did not respond and the reason for this tag failure remains unknown. Two of the six reporting tags released from the manta ray on schedule (180 days, individual M5; 90 days, individual M8), with the remaining four tags releasing prematurely for unknown reasons (retention time 52–140 days). No tags were able to be physically recovered, and four of the tags drifted for an extended period of time at the surface prior to transmitting location data (6 days, M2; 23 days, M4; 5 days, M5; 4 days, M8). Between 44 and 88% of all archived data were retrieved via the Argos satellite system from the six successful tags, of which five provided adequate data for horizontal and vertical movement analyses. Data from the sixth individual, M3, were excluded from further analysis as a result of a lack of light-level data (<10%; **Table 1**).

Horizontal Movement

Satellite tracked *M. alfredi* (three female, two male) moved an average of 8.5 km d^{-1} (range 5.3–12.2 km d^{-1}). The longest recorded track path was 1,632 km for individual M5 over a period of 180 days (GPE3/A; **Table 3**), and the estimated end position of each track varied between 33 and 323 km from the original deployment location (**Figure 3**). The average 50% error radius for geolocated positions estimated across all individuals and HMM models ($n_{\text{positions considered per model}} = 46.8 \pm 6.0$) was 33.1 ± 14.5 km. The size of the areas of core spatial use varied greatly between individuals, with an average core home range area of 13,779 km^2 and extent of home range area of 59,697 km reported from HMM-GPE3 models (ranges of 2,619–32,081 km^2

[2]http://suncalc.net

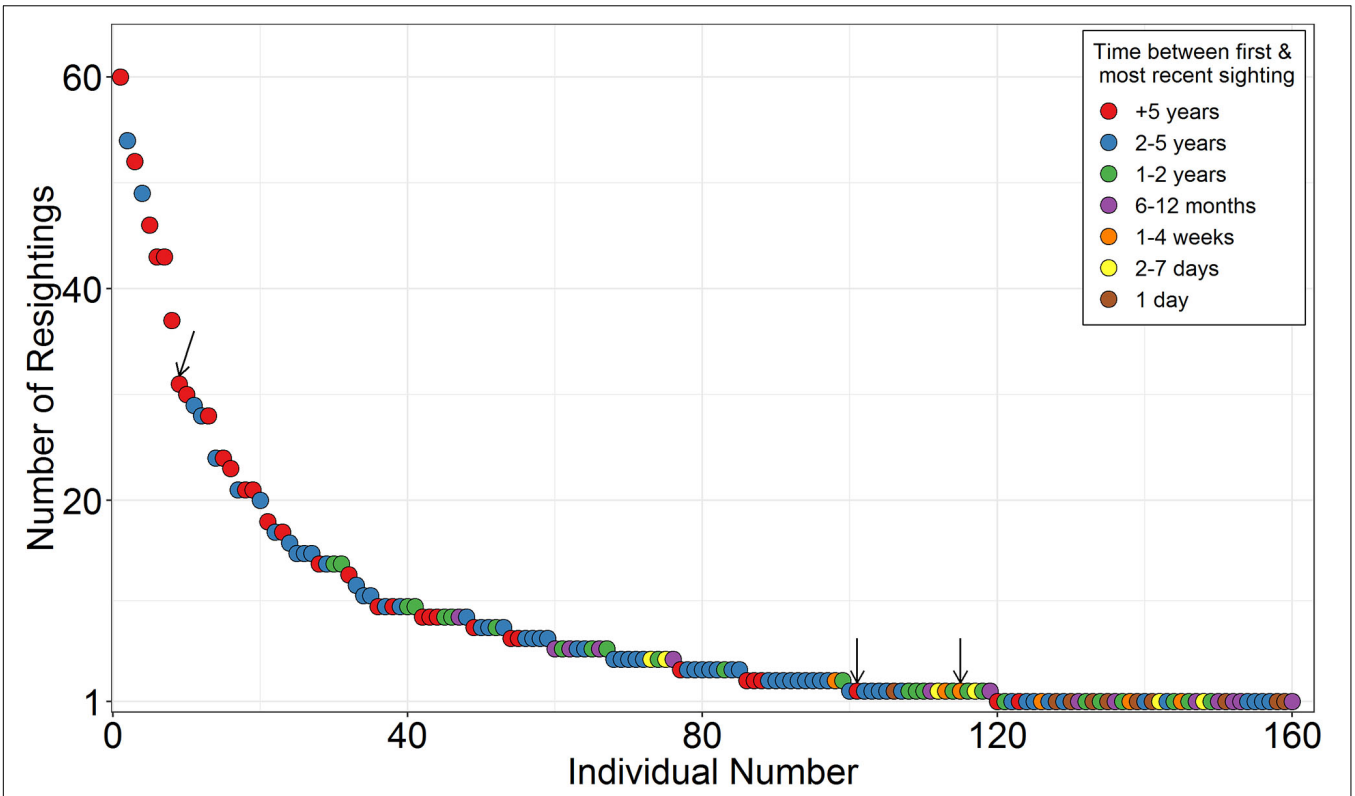

FIGURE 2 | Re-sighting frequency of individual reef manta rays (*Mobula alfredi*) identified using photo-identification techniques in Seychelles (July 2006 to December 2019). Individuals ranked from most to least re-sightings. Time between first sighting and most recent sighting described in the legend. Arrows highlight individuals that were sighted in two of the seven Island Groups of Seychelles. The remaining individuals were always re-sighted at islands and/or atolls within the same Island Group.

TABLE 2 | Sighting histories and locations of eight individual reef manta rays (*Mobula alfredi*) that were tracked in the waters of Seychelles using archival pop-up satellite tags.

Manta ID	First sight (location)	# Resights Pre-tagging	Tag date	# Resights with tag	# Resights post-tag
M1	15 Nov 2012 (D'Arros)	4	27 Nov 2016	0	0
M2	27 Sep 2013 (D'Arros)	6	28 Nov 2016	0	0
M3	20 Nov 2011 (D'Arros)	12	17 Nov 2017	1 (D'Arros)	0
M4	07 Dec 2010 (D'Arros)	22	17 Nov 2017	1 (D'Arros)	1 (Poivre)
M5	18 Nov 2016 (D'Arros)	1	22 Nov 2017	0	0
M6	11 Nov 2016 (St. François)	2	03 Dec 2017	1 (St. François)	1 (St. François)
M7	20 Nov 2011 (St. Joseph Atoll)	17	04 Mar 2019	0	0
M8	22 Nov 2017 (St. Joseph Atoll)	2	04 Mar 2019	0	0

and 12,873–128,680 km^2, respectively). All tagged *M. alfredi* were found to remain within the boundary of the Seychelles Exclusive Economic Zone (EEZ), where the Amirantes Bank represented a key area of use for the majority of individuals. The core areas of space use for tagged individuals across all HMM models spanned just 0.93 ± 0.75% of the Seychelles EEZ, whereas the extents of the home range for individuals encompassed 4.1 ± 3.0% of the EEZ.

The majority (90.6%) of geolocation-derived track positions were estimated to occur within a similar longitudinal range (52.8–54.2°E). Of the 5,154 geolocated positions considered here, a total of 4,045 (78.4%) fell within the same longitudinal range of the Amirantes Group (52.87–53.76°E) and 1,369 (26.0%) fell within the longitudinal range of D'Arros Island and St. Joseph Atoll (53.29–53.37°E; **Figure 4**).

Inclusion of Acoustic Telemetry Data in Geolocation Analysis

The estimated latitudinal range covered by *M. alfredi* ranged from 207 to 594 km within Seychelles, with track paths for individuals tagged in 2016 and 2019 (M1 and M2, and M8, respectively) generally moving in a southerly direction, and track paths for individuals tagged in 2017 (M4 and M5) tending to travel northward. The inclusion of additional location data collected

TABLE 3 | Horizontal and vertical movement metrics for reef manta rays (*Mobula alfredi*) tracked using archival pop-up satellite tags (miniPATs) in Seychelles.

	Metric	M1	M2	M4	M5-GPE3/A	*M5-GPE3*	M8
Individual	PTT	166070	166071	41818	41819	*41819*	49002
Information	Sex	F	F	M	F	*F*	M
	Disc width (m)	3.0	3.6	3.0	3.4	*3.4*	3.0
Horizontal	Pop. dist. (km)	323	193	33	132	*295* (×2.2)	40
Movements	Traveled length (km)	887	278	1,454	1,632	*1,466* (×0.9)	725
	Min. distance/day (km)	8.9	5.3	8.1	12.2	*10.9* (×0.9)	8.1
	Max. lat. range (km)	352	207	551	322	*594* (×1.8)	448
	Core home range (≤50% NUD; km^2)	8,287	2,619	32,081	7,650	*12,281* (×1.6)	13,628
	Extent of home range (≤95% NUD; km^2)	29,094	12,873	128,679	41,040	*73,226* (×1.8)	54,614
Vertical	Max depth (m)	184	280	240	224	–	376
Movements	Min. temp (°C)	14.6	17.1	16.9	12	–	11.7
	Max. temp (°C)	30.7	30.4	30.3	31.7	–	31.8
	Diel depth distribution (*p*)	1.00	1.00	0.52	1.00	–	1.00
	Diel dive depth (*p*)	**<0.001**	0.10	**0.02**	**0.03**	**–**	**<0.001**
	Lunar cycle (*p*)	0.10‡	0.66‡	0.50	**0.04**‡	–	0.38‡

F, female. M, male. Pop. dist., distance between deployment location and estimated end position of track; Max. lat. range, maximum latitudinal range covered by the individual; NUD, normalized utilization distribution; GPE3, geolocated track path including geo-located positions only; GPE3/A, geolocated track path including additional positions recorded by an acoustic tag. Italicized metric data indicate value and difference of M5-GPE3 model to M5-GPE3/A. Diel depth distribution, p-value from two-sample K-S test for difference in depth distribution between day and night. Diel dive depth, p-value from two-sided Wilcoxon rank sum test for difference in average dive depth between day and night. Lunar cycle, p-value for relationship between average night-time depth by individuals and level of moon illumination; ‡ Represents p-value derived from Spearman's rank correlation test. Significant p-values are presented in bold.

from the acoustic tag of M5 in the HMM for this individual (GPE3/A) constricted the latitudinal distance encompassed by the resulting geo-located track path by 45.8% in comparison to the model that considered transmitted light level data alone (GPE3; **Table 3**). Although the total distance moved by M5 during the most-probable track in the GPE3/A model remained similar to that predicted by the GPE3 model (1,632 and 1,466 km, respectively), the GPE3/A model estimated the release location of the tag to be 163 km closer to the tagging location. The home range areas estimated for M5 also differed greatly between models GPE3/A and GPE3, with the core and extent areas constricting by 37.7 and 44.0%, respectively. This change was most notable on the latitudinal axis, with a reduction in latitudinal range of 272 km being observed in model GPE3/A. The percentage of geolocation-estimated positions falling within the latitudinal range of the Amirantes Bank for M5 increased from 44.2% in the GPE3 model, to 69.6% in the GPE3/A model (**Figure 5A**), after accounting for the 481 known locations of M5 within the Amirantes acoustic array between 22 November 2017 and 06 February 2018 (**Figure 5B**).

Vertical Movement

Tagged *M. alfredi* spent an average of 87.4% of their time in the top 50 m of the water column (range 68.0–95.8%; **Figure 6**). Three individuals (M1, female; M2, female; M4, male) remained at depths of less than 120 m, whereas the remaining two individuals (M5, female; M8, male) infrequently occupied deeper depths (>150 m; n = 8 and 20 records, respectively) and reached maximum depths of 213 and 359 m, respectively (**Table 3**). Individuals spent approximately 78.4% of their time at temperatures between 27 and 29°C (range 54.7–94.0%), and 94.0% of their time at temperatures between 24 and 29°C (range 84.5–99.3%; **Figure 6** and **Supplementary Figure S1**). The minimum temperature recorded among tagged individuals was 11.7°C, and the maximum temperature recorded was 31.8°C. Individual M8 reported a lower occupancy within the upper 50 m of the water column (68.0%) and within the temperature range of 27 and 29°C (54.7%) than the other four tagged individuals (mean occupancy of upper 50 m = 91.2 ± 5.7%; mean time spent at 27–29°C = 83.2 ± 9.9%).

Tagged *M. alfredi* spent an average of 79.4 ± 8.4% of their time at depths shallower than the average depth of the Amirantes Bank (40 m; **Figure 6**). This time percentage increased to 92.0 ± 6.0% when depth data were examined relative to the depth of the St. Joseph channel (60 m), located between D'Arros Island and St. Joseph Atoll.

Occupied depth distributions did not differ between the day and night for any individual (K-S test, $p > 0.05$; **Table 3**), or for the pooled dataset (K-S test, $p = 1$; **Supplementary Figure S2**). Average dive depths, however, were deeper during the night than the day for four individuals (two females, two males; W = 2,640, n = 197, $p < 0.001$; W = 5,340, n = 241, p = 0.03; W = 220, n = 74, p = 0.02; W = 2190, n = 176, $p < 0.001$, respectively; **Table 3** and **Supplementary Figure S3**) by an average of 7.80 m (range 5.39–11.64 m). Average dive depths were also deeper during the night (average = 29.48 m) than the day (average = 23.64 m) when individuals were considered collectively (W = 51,700, n = 794, $p < 0.001$). Average nightly dive depth varied slightly with increasing levels of moon illumination for one of the five individuals (female; **Table 3**). Individual M5 dived deeper during a full moon than a new moon (Spearman rank correlation, r_s = 0.20, p = 0.04) at depths between 2.13 and 70.69 m

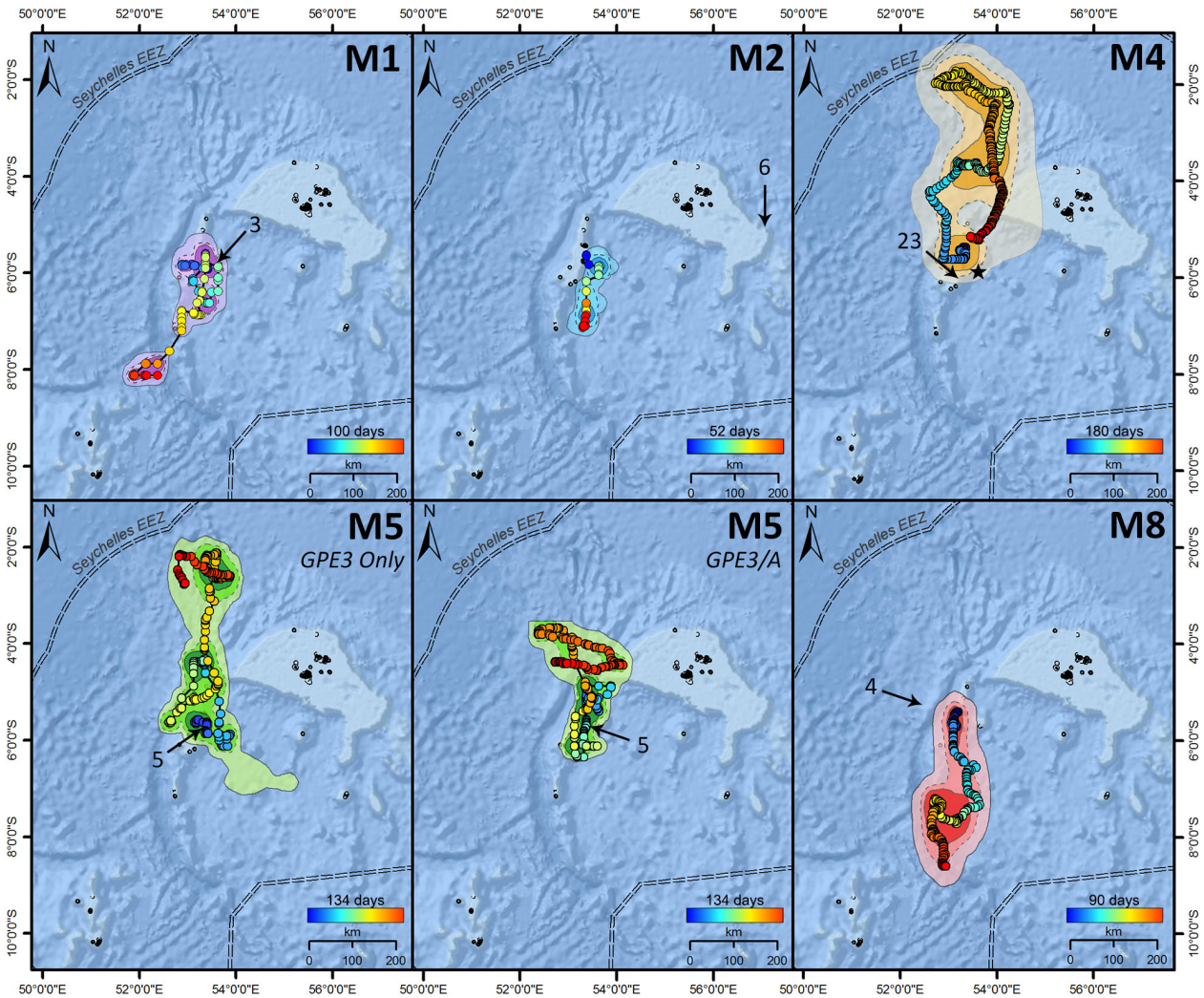

FIGURE 3 | Most-probable tracks for reef manta rays (*Mobula alfredi*) M1, M2, M4, M5, and M8 tagged with archival pop-up satellite tags (miniPATs) at D'Arros Island, Seychelles. For M5, the "GPE3 Only" track was estimated only from archived light, depth, and temperature data, whereas the "GPE3/A" track included an additional 481 acoustic detections from a passive receiver array. Tracks progress from blue to red, with track duration presented above color bars. Arrows indicate the first Argos location of each transmitting tag, and the associated numbers show the number of days that the tag was estimated to have been drifting at the surface prior to transmissions beginning. Home range represented by dark (core area; 50% NUD), medium (75% NUD), and light (extent of area; 95% NUD) color shading, where NUD represents the normalized utilization distribution for the individual. "★" in M4 indicates the location of a re-sighting event recorded 184 days after tag release.

(**Figure 7**). No significant relationships were observed between average nightly dive depth and moon illumination for the other four tagged individuals (**Supplementary Figure S4**), or for the pooled dataset of all individuals (**Supplementary Table S2**).

DISCUSSION

Reef manta rays that were photographed and satellite tagged at D'Arros Island and St. Joseph Atoll displayed restricted movements away from this location. The Amirantes Bank appeared to represent key habitat for all tagged individuals, with photo-identification revealing high site fidelity to the Amirantes Group, and limited inter-island movements of the species across the rest of the Archipelago. Satellite tagged *M. alfredi* spent the majority of their time in the upper 50 m of the water column, with 92% of all depth records found to be shallower than the maximum depth of the St. Joseph Channel (60 m) upon the Amirantes Bank.

Horizontal Movement

Photo-Identification

Photo-identification data suggested that *M. alfredi* display high site fidelity to sighting locations, and high residency within the Island Groups of Seychelles, with almost two-thirds of identified individuals being re-sighted on at least one occasion throughout the Archipelago. At D'Arros Island at St. Joseph Atoll, individuals were resighted up to 60 times over 9.5 years, with variable periods

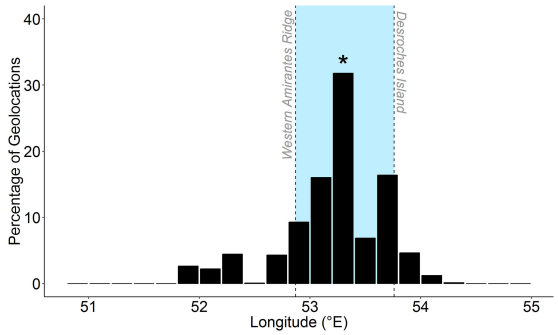

FIGURE 4 | Percentage of longitude estimates among five geo-located satellite tracks of reef manta rays (*Mobula alfredi*) in Seychelles. Blue shading represents longitudinal range of the Amirantes Group. Asterisk represents longitude at tagging location (D'Arros Island).

of absence occurring between re-sightings. Within the Amirantes Group, 17 individuals were sighted at both D'Arros Island and either Desroches Atoll or Poivre Atoll. Such movements between the islands of the Amirantes have been recorded previously using passive acoustic telemetry (Peel et al., 2019b), and highlight the site fidelity that *M. alfredi* displays to locations in the region. Photo-identification also found evidence of only three movements of >200 km being recorded between D'Arros Island (Amirantes Group) and St, François Atoll (Alphonse Group) in the past 3 years, representing the only confirmed movements of *M. alfredi* between any Island Groups of Seychelles to-date. Additionally, two of the eight satellite-tagged individuals were resighted close to their tagging location after shedding their tags. Similar levels of site fidelity have been reported for *M. alfredi* at other localities using photo-identification, with food availability and deep-water barriers to movement thought to contribute to the extended site occupancy of individuals at key aggregation sites (Couturier et al., 2011; Deakos et al., 2011; Marshall et al., 2011; Germanov and Marshall, 2014). In Seychelles, the bathymetry of the Amirantes Bank may drive increased zooplankton accumulation in an otherwise oligotrophic region, subsequently generating reliable food sources for *M. alfredi* and contributing to the observed residency of this species at the Amirantes Group (Gove et al., 2016; Peel et al., 2019b). Continued efforts to monitor the patterns of movement of *M. alfredi* in Seychelles using photo-identification will provide additional insight into the distribution and connectivity of this population, and strengthen the current understanding of residency and site fidelity in this species. Furthermore, the impact of these data will be maximized if records can be collected by a network of citizen scientists throughout the region. Such a network will assist in overcoming the challenges associated with surveying the substantial area encompassed by the Seychelles EEZ and the large distances that separate islands of the archipelago (maximum 1,200 km), which were encountered in the present study.

Satellite Telemetry

The suggestion of prolonged residency of *M. alfredi* to the Island Groups of Seychelles provided by the photo-identification component of this study was supported by satellite tagging, and further emphasized by the latitudinal constriction observed in the geo-located track for the individual that was also acoustically tagged. All satellite tagged *M. alfredi* remained in close proximity to the Amirantes Bank while they were tracked, and no individual was recorded to exit the Seychelles EEZ. The residency of tagged *M. alfredi* to the Amirantes Group, and potentially to D'Arros Island and St. Joseph Atoll, was highlighted by the frequency at which track positions were estimated to occur within the latitudinal and longitudinal ranges of these locations. Similar patterns of restricted movement have been reported for satellite tagged *M. alfredi* elsewhere (Jaine et al., 2014; Braun et al., 2015; Kessel et al., 2017; Carlisle et al., 2019; Andrzejaczek et al., 2020). Individuals in eastern Australia, for example, dispersed up to 520 km from their tagging location (Jaine et al., 2014), but all were observed to travel back toward this location prior to the end of their track. A higher level of site fidelity was noted for *M. alfredi* tagged in the Red Sea, where the repeated visitation of individuals to a coastal aggregation area was recorded and regional movements occurred within 200 km of the tagging site (Braun et al., 2015; Kessel et al., 2017). The similar spatial scales of tracks reported for *M. alfredi* across these other locations, and as now recorded in Seychelles, supports the hypothesis that limited dispersal and high residency to aggregation areas are characteristic of this species.

The patterns of movement of male (n = 2) and female (n = 3) *M. alfredi* were considered collectively in this study. Three of the five miniPATs deployed on male *M. alfredi* failed to report a reliable dataset, so a comparison between the movement patterns of the sexes was not attempted. Tag failure has been reported in numerous studies of the movement ecology of elasmobranchs (Braun et al., 2015; Ferreira et al., 2015; Skomal et al., 2017; Domeier et al., 2019). Indeed, it is an unavoidable component of telemetry-based research given the suite of factors in the marine environment that can lead to tag damage, loss or computational error (Hammerschlag et al., 2011). The deployment of a larger number of tags on *M. alfredi* in Seychelles in the future will reduce the impact of these three tag failures on the cumulative dataset for this region. Additional tags may also provide insight into the frequency of occurrence of large-scale movements by *M. alfredi* throughout the country, and the extent of connectivity that exists between the population of *M. alfredi* in Seychelles and other populations identified elsewhere in the Indian Ocean (e.g., Chagos, Maldives, Mozambique; Marshall et al., 2011; Stevens, 2016; Carlisle et al., 2019; Andrzejaczek et al., 2020).

All five of the tracks examined in this study were associated with tags deployed on mature *M. alfredi.* Mature individuals were hypothesized to travel further than immature individuals at the time of tag deployment. This was because of the reduced energy requirements that are associated with travel for larger fishes (Ware, 1978) and the observation of size-based variation in movement patterns in other elasmobranch species (Bansemer and Bennett, 2011; Chapman et al., 2015). Larger *M. alfredi* were therefore anticipated to encompass the widest possible home range for this species in Seychelles, and were selectively targeted during tagging. Juvenile *M. alfredi* were

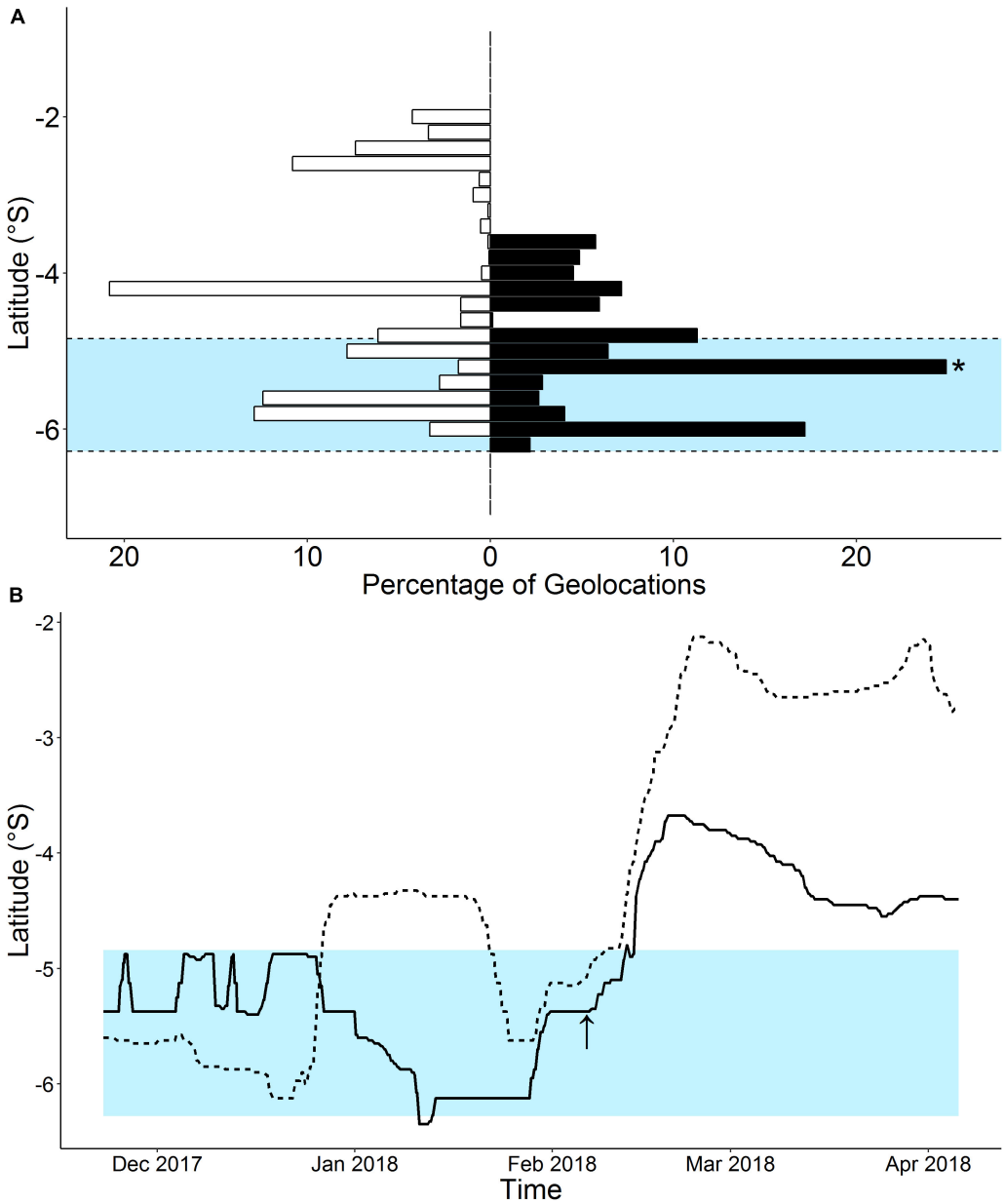

FIGURE 5 | Percentage of total latitude estimates calculated for a geo-located satellite track of a reef manta ray (*Mobula alfredi*; individual M5) in Seychelles by a hidden Markov model (HMM) considering either archived environmental data only (GPE3; white bars), or archived environmental data and 481 known locations retrieved from an acoustic receiver array (GPE3/A; black bars; **A**). Asterisk represents longitude at tagging location (−5.409°S; D'Arros Island). Estimated latitude over time also presented **(B)** for HMM models with (GPE3/A; solid line) and without (GPE3; dashed line) acoustic data. Blue shading in both panels represents latitudinal range of the Amirantes Group. Arrow indicates time of last recorded acoustic detection of individual.

subsequently confirmed to display a higher level of residency and site fidelity to D'Arros Island than larger individuals monitored passively through an acoustic receiver array in the Amirantes Group (Peel et al., 2019b). For this reason, future studies aiming to deploy additional satellite tags on *M. alfredi* in Seychelles to further examine home range size and the potential for large-scale (>200 km) movements in this population should continue to focus efforts on mature males and females, and endeavor to tag individuals at other Island Groups. This will facilitate a comparison of movement patterns between the sexes (Sequeira et al., 2019) and across a wider region of Seychelles.

Influence of Acoustic Telemetry Data on Modeled Patterns of Movement

The inclusion of acoustic detection data in the HMM of one satellite-tagged individual in this study significantly restricted the latitudinal range encompassed by the associated track by

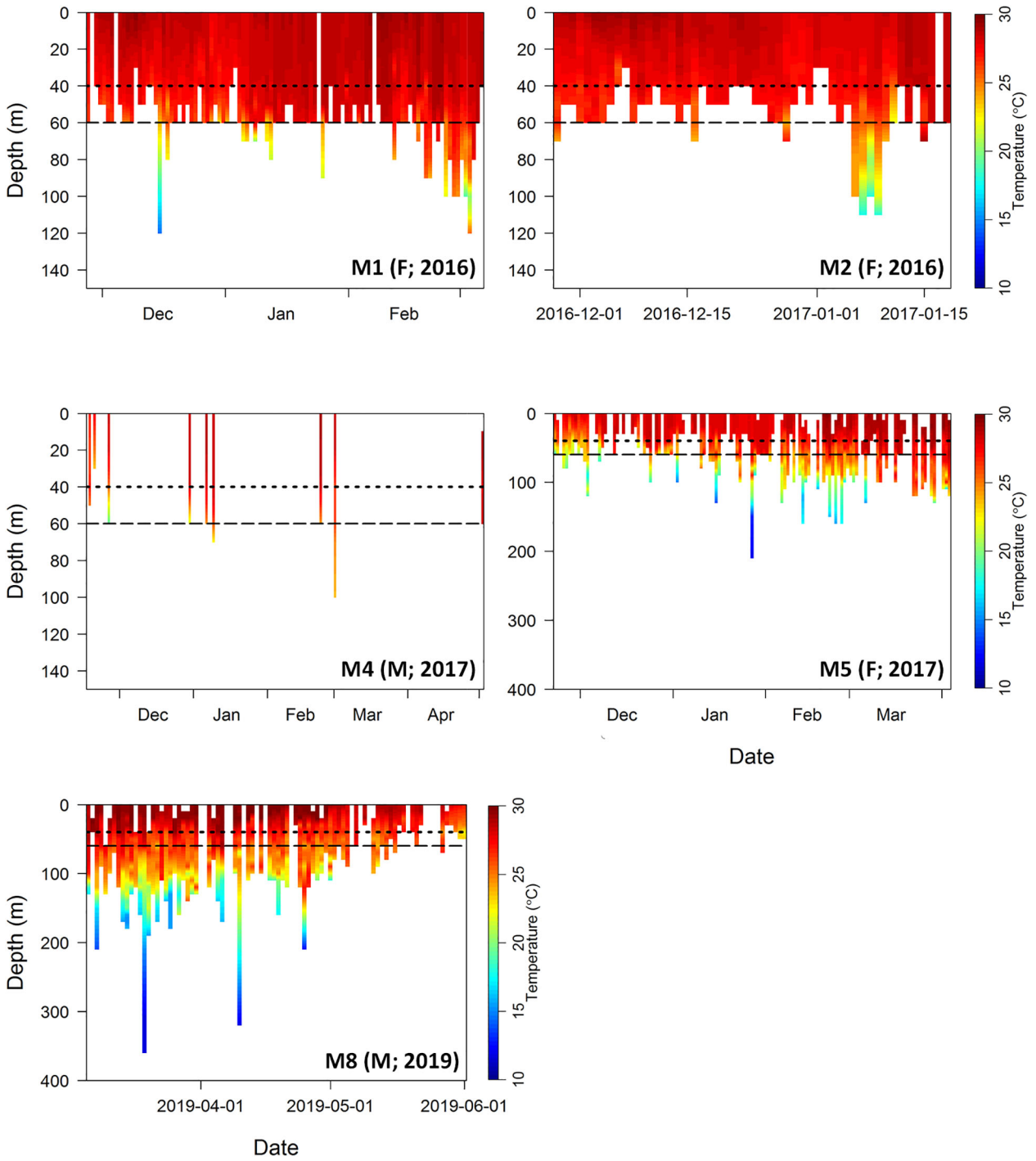

FIGURE 6 | Combined depth and temperature profiles for five reef manta rays (*Mobula alfredi*) tagged with archival pop-up satellite tags in Seychelles. Data interpolated from archived time series data (10 min intervals) for each day of data retrieved per tag. Depth data presented in 10 m bins and temperature data interpolated at a resolution of 0.5°C. Gaps indicate data that were not retrieved from the tag prior to tag battery depletion. Manta identification number (M*), sex (F, female; M, male), and year of tag deployment indicated in lower right of each panel. Dotted line represents average depth of the Amirantes Bank (40 m), and dashed line represents average depth of St. Joseph Channel (60 m) located between D'Arros Island and St. Joseph Atoll. Note variable depth scale on *y*-axis.

reducing geolocated-position error from an approximate radius of 30.1 km to only 165 m. In addition to highlighting the magnitude of error present in the HMM models that considered geolocation position estimates alone, the inclusion of acoustic detection data also increased the frequency at which the position estimates for this individual fell within the range of the Amirantes

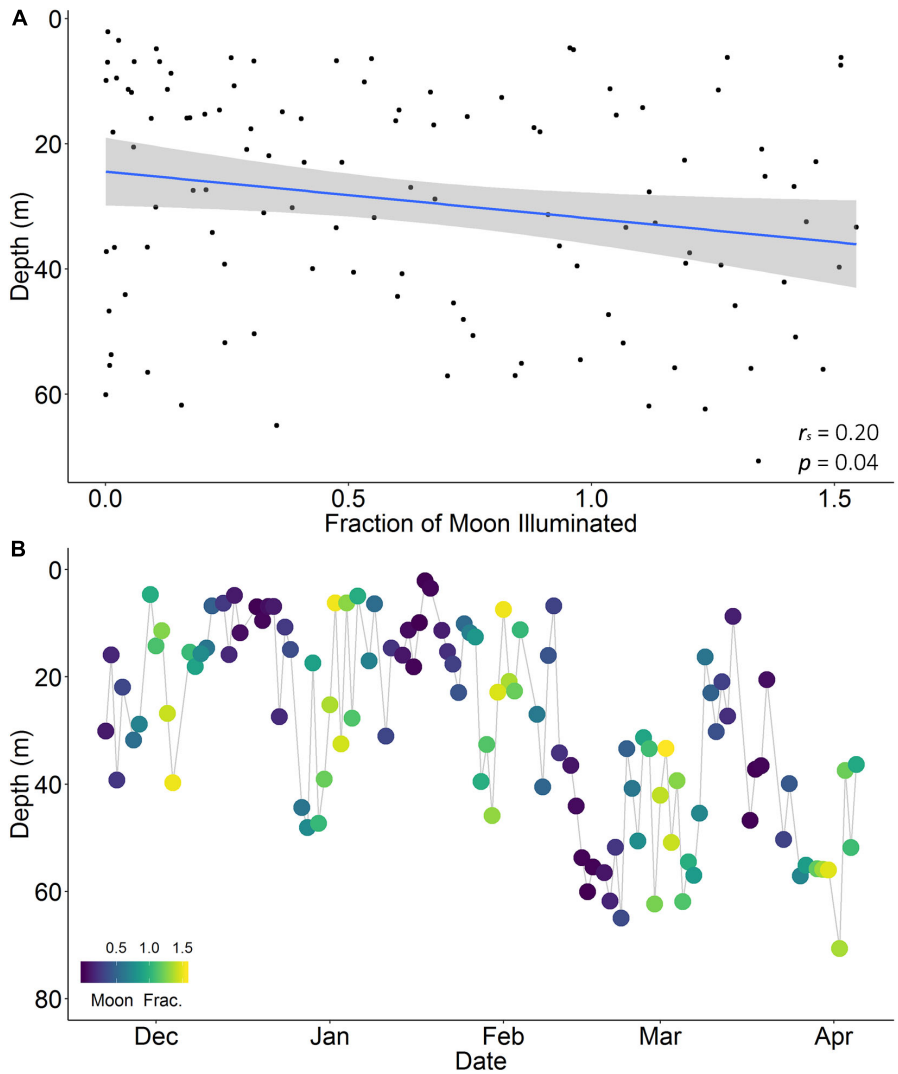

FIGURE 7 | Nightly average dive depth relative to moon illumination (arcsine transformed; **A**) and over time (November 2017 to April 2018; **B**) for a female reef manta ray (*Mobula alfredi*; M5) tagged with pop-up archival satellite tag in Seychelles. Blue line indicates direction of relationship with moon illumination based on a Spearman's rank correlation. Gray shading indicates 95% confidence interval. Note that this is the only individual of five to display a significant relationship.

Group. Geolocation errors are known to increase with increasing proximity to the equator because of the lack of seasonal variation in the timing of sunrise and sunset, and the consistency of sea surface temperature throughout the equatorial zone (Nielsen et al., 2006; Nielsen and Sibert, 2007; Braun et al., 2015, 2018a). Given this outcome, future studies of the movement patterns of *M. alfredi* and other marine megafauna species in Seychelles and elsewhere in the equatorial zone should consider using alternative satellite tag types. For example, tags that incorporate GPS and Argos technology alongside geolocation capabilities (SPLASH or GPS Fastloc tags; Doherty et al., 2017), or fin-mounted or towed tags that provide live updates of location via satellite (SPOT tags; Kessel et al., 2017). Regardless of whether these studies focus on the fine-scale patterns of habitat use of juveniles and adults, or on the broader movement patterns of adults specifically, such tags may also help to increase the amount of archived high-resolution data that can be transmitted via satellite; a useful function in remote locations such as Seychelles, where land is scarce (459 km^2 of the 1,340,000 km^2 EEZ) and detached satellite tags are unlikely to wash ashore for easy retrieval, as has occurred elsewhere (Braun et al., 2014; Jaine et al., 2014).

Vertical Movement

Little variation was observed in the vertical movement patterns of *M. alfredi* tagged at D'Arros Island. Individuals spent the majority of their time in the top 50 m of the water column at temperatures between 27 and 29°C, with only two individuals infrequently reaching mesopelagic depths (>200 m; M5, two records; M8, six records), despite the ability of the species to reach depths of over 600 m (Lassauce et al., 2020). Average dive depth increased at night for four of the five individuals that were successfully tagged, a behavior consistent with observations from the pooled dataset

and the results of similar studies in the Red Sea (Braun et al., 2014). Diel shifts in patterns of vertical habitat use by manta rays and other elasmobranchs have been attributed to foraging behavior (Couturier et al., 2013; Burgess et al., 2016; Lassauce et al., 2020) and/or predator aversion (Gliwicz, 1986; Hays, 2003; Webster et al., 2015). Given the relatively coarse nature of the movement data retrieved in this study, however, additional tag deployments on *M. alfredi* in Seychelles will be required to further explore the mechanisms underlying the patterns of vertical habitat use by this species.

A weak relationship between average nightly dive depth and moon illumination level was noted for one of the five *M. alfredi* successfully tracked in this study, with the individual diving slightly deeper during a full moon than a new moon. In the Red Sea, dive depth was found to increase with moon illumination for *M. alfredi* when individuals moved from inshore waters (<15 km from coastline; $R^2 = 0.10$, $p = 0.01$) to offshore waters (>15 km from coastline; $R^2 = 0.503$, $p < 0.001$; Braun et al., 2014). The increased illumination of the full moon is thought to restrict the extent of diel vertical migration of zooplankton through the water column in these deeper, offshore locations, subsequently altering the vertical movement patterns of foraging *M. alfredi* (Hays, 2003; Couturier et al., 2013; Braun et al., 2014). It is, therefore, possible that the weak or absent influence of moon illumination on the dive profiles of *M. alfredi* reported here is a result of the residency displayed by individuals to the typically shallow Amirantes Bank (average depth 40 m; Stoddart et al., 1979), where increased prey availability may reduce their need to forage at deep, offshore sites during the night. Future tagging efforts that allow for the collection of higher resolution depth and position data for *M. alfredi* over multiple lunar cycles are required to confirm this hypothesis, and to quantify the extent to which vertical movement patterns vary at an individual level within this population (Sequeira et al., 2019).

The consistent and shallow (<50 m) habitat use of *M. alfredi* increases the likelihood of individuals encountering anthropogenic threats (Dulvy et al., 2014). These include, but are not limited to, boat strikes, accidental entanglements in fishing gear, and targeted fishing practices (Heinrichs et al., 2011; Croll et al., 2016; Stewart et al., 2018; McGregor et al., 2019). The reliable aggregation of individuals at specific locations in Seychelles, particularly within the Amirantes Group (Peel et al., 2019b), further increases these risks for *M. alfredi*. The predictability of these aggregation events in both time and space increases the risk of exploitation for a substantial number of individuals. Although a dedicated mobulid fishery does not currently exist in Seychelles (Temple et al., 2019), the large impact of small-scale fisheries on elasmobranch populations in the south-western Indian Ocean region is becoming increasingly apparent (Temple et al., 2018, 2019). In Mozambique, for example, sightings of *M. alfredi* were recorded to decline by 98% between 2003 and 2016 (Rohner et al., 2017). Should the demand for mobulid products—specifically gill plates (Whitcraft et al., 2014; Lawson et al., 2017; O'Malley et al., 2017)—increase in the south-western Indian Ocean, it is highly likely to increase the susceptibility of the Seychelles *M. alfredi* population to exploitation and decline (Temple et al., 2019).

In the absence of national-scale protective legislature for this globally "vulnerable" species, the aforementioned anthropogenic threats raise concerns regarding the longevity of *M. alfredi* aggregations throughout Seychelles and emphasize the importance of the Marine Spatial Plan announced by the Seychellois Government in 2020 to this remote population. The 13 MPAs encompassing this scheme, including one surrounding D'Arros Island and St. Joseph Atoll (Minister of Environment, 2020), span 410,000 km^2 (30%) of the Seychelles EEZ and represent a significant step forward in the conservation of *M. alfredi* in the Western Indian Ocean. The extent of benefits afforded to *M. alfredi* by these MPAs, however, will depend on the regulations incorporated into their management. Both the prohibition of fishing for manta rays and the adherence to protocols regarding human–manta ray interactions for tourism (Venables et al., 2016; Murray et al., 2019), for example, would benefit *M. alfredi* at these sites, if enforced. Ultimately, by encompassing important habitat for *M. alfredi* at D'Arros Island and St. Joseph Atoll, these MPAs provide an opportunity to conserve a key aggregation site for the Seychelles population, until a targeted, national-scale management strategy can be developed and implemented for the species.

CONCLUSION

Photo-identification, and satellite and acoustic telemetry, have revealed that *M. alfredi* photographed and tagged at D'Arros Island and St. Joseph Atoll were largely resident to the Amirantes Group of Seychelles. Tagged individuals spent the majority of the time that they were tracked in the upper 50 m of the water column, likely over the shallow Amirantes Bank, where they may face increasing exposure to anthropogenic threats from small- and large-scale fisheries in the Western Indian Ocean in the future. These findings suggest that the recent establishment of an MPA at D'Arros Island and St. Joseph Atoll, and more broadly across the Amirantes Bank as a whole, will benefit *M. alfredi* conservation efforts in Seychelles, given appropriate regulations regarding manta ray fishing and tourism practices are enforced. Furthermore, should *M. alfredi* occasionally leave the boundary of the Seychelles EEZ and travel to other aggregation areas identified for the species in the region (e.g., Chagos, Maldives, Mozambique), it is likely that such protective measures in Seychelles would also benefit conservation efforts more broadly across the Western Indian Ocean. Continued monitoring of the movement patterns of this remote population across the archipelago will be crucial to the assessment of regional (i.e., within Island Group) and national scale management strategies for this globally vulnerable species.

DATA AVAILABILITY STATEMENT

The datasets generated for this study are available on request to the corresponding author.

ETHICS STATEMENT

This animal study was reviewed and approved by the Seychelles Bureau of Standards, the Seychelles Ministry of Environment, Energy and Climate Change, Islands Development Company, Alphonse Foundation, and The University of Western Australia (RA/3/100/1480).

AUTHOR CONTRIBUTIONS

LP, GS, RD, SC, JN, and MM contributed to the design and implementation of the research. LP, GS, RD, CK, and JN conducted fieldwork and assisted with data collection. LP analyzed the data and prepared associated figures. LP, RD, and MM drafted the manuscript. All authors provided feedback on the manuscript and gave final approval for publication.

FUNDING

This study was funded by the Save Our Seas Foundation (SOSF) and supported by The Manta Trust, The University of Western Australia, and the Australian Institute of Marine Science. Field work was supported by the SOSF-D'Arros Research Centre, Island Conservation Society (ICS), Alphonse Foundation, Islands Development Company, Blue Safari, the Alphonse Island Lodge, and the UWA Postgraduate Student's Association.

ACKNOWLEDGMENTS

We would like to thank Justin Blake (SOSF), Luke Gordon (SOSF/Manta Trust), Ariadna Fernandez (ICS), Christopher Narty (ICS), and Lucy Martin (Blue Safari) for their assistance in the field. We would also like to thank the Head Office Management Team of ICS for their support in coordinating and facilitating the administrative measures associated with this research. Additionally, we thank Dr. Luciana Ferreira and Amelia Armstrong for comments on the geolocation analyses used in this study. Finally, we thank two reviewers for their valuable feedback on an earlier version of this manuscript.

SUPPLEMENTARY MATERIAL

The Supplementary Material for this article can be found online at: https://www.frontiersin.org/articles/10.3389/fmars.2020.00558/full#supplementary-material

REFERENCES

Agafonkin, V., and Thieurmel, B. (2018). *suncalc: Compute Sun Position, Sunlight Phases, Moon Position and Lunar Phase: R Package Version 0.4*.

Andrzejaczek, S., Chapple, T. K., Curnick, D. J., Carlisle, A. B., Castleton, M., Jacoby, D. M. P., et al. (2020). Individual variation in residency and regional movements of reef manta rays *Mobula alfredi* in a large marine protected area. *Mar. Ecol. Prog. Ser.* 639, 137–153. doi: 10.3354/meps13270

Andrzejaczek, S., Gleiss, A. C., Jordan, L. K., Pattiaratchi, C. B., Howey, L. A., Brooks, E. J., et al. (2018). Temperature and the vertical movements of oceanic whitetip sharks, *Carcharhinus longimanus*. *Sci. Rep.* 8:8351. doi: 10.1038/s41598-018-26485-3

Armstrong, A. O., Armstrong, A. J., Bennett, M. B., Richardson, A. J., Townsend, K. A., and Dudgeon, C. L. (2019). Photographic identification and citizen science combine to reveal long distance movements of individual reef manta rays *Mobula alfredi* along Australia's east coast. *Mar. Biodivers. Rec.* 12:14.

Bansemer, C. S., and Bennett, M. B. (2011). Sex- and maturity-based differences in movement and migration patterns of grey nurse shark, *Carcharias taurus*, along the eastern coast of Australia. *Mar. Freshw. Res.* 62, 596–606. doi: 10.1071/MF10152

Bates, D., Maechler, M., Bolker, B., and Walker, S. (2015). Fitting linear mixed-effects models using lme4. *J. Stat. Softw.* 67, 1–48. doi: 10.18637/jss.v067.i01

Bauer, R. (2018). *RchivalTag: Analyzing Archival Tagging Data: R Package Version 0.0.7*.

Braun, C. D., Galuardi, B., and Thorrold, S. R. (2018a). HMMoce: an R package for improved geolocation of archival-tagged fishes using a hidden Markov method. *Methods Ecol. Evol.* 9, 1212–1220. doi: 10.1111/2041-210x.12959

Braun, C. D., Skomal, G. B., and Thorrold, S. R. (2018b). Integrating archival tag data and a high-resolution oceanographic model to estimate basking shark (*Cetorhinus maximus*) movements in the Western Atlantic. *Front. Mar. Sci.* 5:25. doi: 10.3389/fmars.2018.00025

Braun, C. D., Skomal, G. B., Thorrold, S. R., and Berumen, M. L. (2014). Diving behavior of the reef manta ray links coral reefs with adjacent deep pelagic habitats. *PLoS One* 9:e88170. doi: 10.1371/journal.pone.0088170

Braun, C. D., Skomal, G. B., Thorrold, S. R., and Berumen, M. L. (2015). Movements of the reef manta ray (*Manta alfredi*) in the Red Sea using satellite and acoustic telemetry. *Mar. Biol.* 162, 2351–2362. doi: 10.1007/s00227-015-2760-3

Burgess, K. B., Couturier, L. I. E., Marshall, A. D., Richardson, A. J., Weeks, S. J., and Bennett, M. B. (2016). *Manta birostris*, predator of the deep? Insight into the diet of the giant manta ray through stable isotope analysis. *R. Soc. Open Sci.* 3:160717. doi: 10.1098/rsos.160717

Calenge, C. (2006). The package "adehabitat" for the R software: a tool for the analysis of space and habitat use by animals. *Ecol. Model* 197, 516–519. doi: 10.1016/j.ecolmodel.2006.03.017

Canese, S., Cardinali, A., Romeo, T., Giusti, M., Salvati, E., Angiolillo, M., et al. (2011). Diving behavior of the giant devil ray in the Mediterranean Sea. *Endanger Species Res.* 14, 171–176. doi: 10.3354/esr00349

Carlisle, A. B., Tickler, D., Dale, J. J., Ferretti, F., Curnick, D. J., Chapple, T. K., et al. (2019). Estimating space use of mobile fishes in a large marine protected area with methodological considerations in acoustic array design. *Front. Mar. Sci.* 6:256. doi: 10.3389/fmars.2019.00256

Chapman, D. D., Feldheim, K. A., Papastamatiou, Y. P., and Hueter, R. E. (2015). There and back again: a review of residency and return migrations in sharks, with implications for population structure and management. *Annu. Rev. Mar. Sci.* 7, 547–570. doi: 10.1146/annurev-marine-010814-015730

Clark, T. B. (2010). *Abundance, Home Range, and Movement Patterns of Manta Rays (Manta alfredi, M. bistrosis)*. Hawai'i: Mânoa.

Cochran, J. E. M., Braun, C. D., Cagua, E. F., Campbell, M. F. Jr., Hardenstine, R. S., Kattan, A., et al. (2019). Multi-method assessment of whale shark (*Rhincodon typus*) residency, distribution, and dispersal behavior at an aggregation site in the Red Sea. *PLoS One* 14:e0222285. doi: 10.1371/journal.pone.0222285

Couturier, L. I. E., Dudgeon, C. L., Pollock, K. H., Jaine, F. R. A., Bennett, M. B., Townsend, K. A., et al. (2014). Population dynamics of the reef manta ray *Manta alfredi* in eastern Australia. *Coral Reefs* 33, 329–342. doi: 10.1007/s00338-014-1126-5

Couturier, L. I. E., Jaine, F. R. A., Townsend, K. A., Weeks, S. J., Richardson, A. J., and Bennett, M. B. (2011). Distribution, site affinity and regional movements of the manta ray, *Manta alfredi* (Krefft, 1868), along the east coast of Australia. *Mar. Freshw. Res.* 62, 628–637. doi: 10.1071/MF10148

Couturier, L. I. E., Marshall, A. D., Jaine, F. R. A., Kashiwagi, T., Pierce, S. J., Townsend, K. A., et al. (2012). Biology, ecology and conservation of the Mobulidae. *J. Fish Biol.* 80, 1075–1119. doi: 10.1111/j.1095-8649.2012.03264.x

Couturier, L. I. E., Newman, P., Jaine, F. R. A., Bennett, M. B., Venables, W. N., Cagua, E. F., et al. (2018). Variation in occupancy and habitat use of *Mobula alfredi* at a major aggregation site. *Mar. Ecol. Prog. Ser.* 599, 125–145. doi: 10.3354/meps12610

Couturier, L. I. E., Rohner, C. A., Richardson, A. J., Marshall, A. D., Jaine, F. R. A., Bennett, M. B., et al. (2013). Stable isotope and signature fatty acid analyses suggest reef manta rays feed on demersal zooplankton. *PLoS One* 8:e77152. doi: 10.1371/journal.pone.0077152

Croll, D. A., Dewar, H., Dulvy, N. K., Fernando, D., Francis, M. P., Galván-Magaña, F., et al. (2016). Vulnerabilities and fisheries impacts: the uncertain future of manta and devil rays. *Aquat. Conserv.* 26, 562–575. doi: 10.1002/aqc.2591

Deakos, M. H., Baker, J., and Bejder, L. (2011). Characteristics of a manta ray (*Manta alfredi*) population off Maui, Hawaii, and implications for management. *Mar. Ecol. Prog. Ser.* 429, 245–260. doi: 10.3354/meps09085

Dewar, H. (2002). *Preliminary Report: Manta Harvest in Lamakera, Oceanside*. Oceanside, CA: Pfleger Institute of Environmental Research.

Doherty, P. D., Baxter, J. M., Gell, F. R., Godley, B. J., Graham, R. T., Hall, G., et al. (2017). Long-term satellite tracking reveals variable seasonal migration strategies of basking sharks in the north-east Atlantic. *Sci. Rep.* 7:42837. doi: 10.1038/srep42837

Domeier, M. L., Ortega-Garcia, S., Nasby-Lucas, N., and Offield, P. (2019). First marlin archival tagging study suggests new direction for research. *Mar. Freshw. Res.* 70, 603–608. doi: 10.1071/MF18160

Dulvy, N. K., Fowler, S. L., Musick, J. A., Cavanagh, R. D., Kyne, P. M., Harrison, L. R., et al. (2014). Extinction risk and conservation of the world's sharks and rays. *eLife* 3:e00590. doi: 10.7554/eLife.00590

Dwyer, R. G., Krueck, N. C., Udyawer, V., Heupel, M. R., Chapman, D., Pratt, H. L. Jr., et al. (2020). Individual and population benefits of marine reserves for reef sharks. *Curr. Biol.* 30, 1–10. doi: 10.1016/j.cub.2019.12.005

Ferreira, L. C., Thums, M., Heithaus, M. R., Barnett, A., Abrantes, K. G., Holmes, B. J., et al. (2017). The trophic role of a large marine predator, the tiger shark *Galeocerdo cuvier*. *Sci. Rep.* 7:7641. doi: 10.1038/s41598-017-07751-2

Ferreira, L. C., Thums, M., Meeuwig, J. J., Vianna, G. M. S., Stevens, J., McAuley, R., et al. (2015). Crossing latitudes — long-distance tracking of an apex predator. *PLoS One* 10:e0116916. doi: 10.1371/journal.pone.0116916

Germanov, E. S., and Marshall, A. D. (2014). Running the gauntlet: regional movement patterns of *Manta alfredi* through a complex of parks and fisheries. *PLoS One* 9:e110071. doi: 10.1371/journal.pone.0110071

Gliwicz, Z. M. (1986). A lunar cycle in zooplankton. *Ecology* 67, 883–897. doi: 10.2307/1939811

Gove, J. M., McManus, M. A., Neuheimer, A. B., Polovina, J. J., Drazen, J. C., Smith, C. R., et al. (2016). Near-island biological hotspots in barren ocean basins. *Nat. Commun.* 7:10581. doi: 10.1038/ncomms10581

Hammerschlag, N., Gallagher, A., and Lazarre, D. (2011). A review of shark satellite tagging studies. *J. Exp. Mar. Biol. Ecol.* 398, 1–8. doi: 10.1016/j.jembe.2010.12.012

Hamylton, S., Spencer, T., and Hagan, A. B. (2012). "Coral reefs and reef islands of the Amirantes Archipelago, Western Indian Ocean," in *Seafloor Geomorphology as Benthic Habitat: GeoHAB Atlas of Seafloor Geomorphic Features and Benthic Habitats*, eds P. T. Harris, and E. K. Baker, (London: Elsevier), 341–348.

Hays, G. C. (2003). A review of the adaptive significance and ecosystem consequences of zooplankton diel vertical migrations. *Hydrobiologia* 503, 163–170. doi: 10.1023/B:HYDR.0000008476.23617.b0

Hays, G. C., Ferreira, L. C., Sequeira, A. M. M., Meekan, M. G., Duarte, C. M., Bailey, H., et al. (2016). Key questions in marine megafauna movement ecology. *Trends Ecol. Evol.* 31, 463–475. doi: 10.1016/j.tree.2016.02.015

Heinrichs, S., O'Malley, M., Medd, H., and Hilton, P. (2011). *Manta Ray of Hope: Global Threat to Manta and Mobula Rays*. San Francisco, CA: Manta Ray of Hope Project.

Heupel, M. R., Semmens, J., and Hobday, A. (2006). Automated acoustic tracking of aquatic animals: scales, design and deployment of listening station arrays. *Mar. Freshw. Res.* 57, 1–13.

Horne, J. S., Garton, E. O., Krone, S. M., and Lewis, J. S. (2007). Analyzing animal movements using Brownian bridges. *Ecology* 88, 2354–2363. doi: 10.1890/06-0957.1

Jaine, F. R. A., Rohner, C. A., Weeks, S. J., Couturier, L. I. E., Bennett, M. B., Townsend, K. A., et al. (2014). Movements and habitat use of reef manta rays off eastern Australia: offshore excursions, deep diving and eddy affinity revealed by satellite telemetry. *Mar. Ecol. Prog. Ser.* 510, 73–86. doi: 10.3354/meps10910

Kashiwagi, T., Marshall, A. D., Bennett, M. B., and Ovenden, J. R. (2011). Habitat segregation and mosaic sympatry of the two species of manta ray in the Indian and Pacific Oceans: *Manta alfredi* and *M. birostris*. *Mar. Biodivers. Rec.* 4:e53.

Kessel, S. T., Elamin, N. A., Yurkowski, D. J., Chekchak, T., Walter, R. P., Klaus, R., et al. (2017). Conservation of reef manta rays (*Manta alfredi*) in a UNESCO World Heritage Site: large-scale island development or sustainable tourism? *PLoS One* 12:e0185419. doi: 10.1371/journal.pone.0185419

Kitchen-Wheeler, A.-M. (2010). Visual identification of individual manta ray (*Manta alfredi*) in the Maldives Islands, Western Indian Ocean. *Mar. Biol. Res.* 6, 351–363. doi: 10.1080/17451000903233763

Kneebone, J., Chisholm, J., and Skomal, G. (2014). Movement patterns of juvenile sand tigers (*Carcharias taurus*) along the east coast of the USA. *Mar. Biol.* 161, 1149–1163. doi: 10.1007/s00227-014-2407-9

Lassauce, H., Chateau, O., Erdmann, M., and Wantiez, L. (2020). Diving behavior of the reef manta ray (*Mobula alfredi*) in New Caledonia: more frequent and deeper night-time diving to 672 meters. *PLoS One* 15:e0228815. doi: 10.1371/journal.pone.0228815

Lawson, J. M., Fordham, S. V., O'Malley, M. P., Davidson, L. N. K., Walls, R. H. L., Heupel, M. R., et al. (2017). Sympathy for the devil: a conservation strategy for devil and manta rays. *PeerJ* 5:e3027. doi: 10.7717/peerj.3027

Lea, J. S. E., Humphries, N. E., von Brandis, R. G., Clarke, C. R., and Sims, D. W. (2016). Acoustic telemetry and network analysis reveal the space use of multiple reef predators and enhance marine protected area design. *Proc. R. Soc. Lond. B. Biol. Sci.* 283:20160717. doi: 10.1098/rspb.2016.0717

Letessier, T. B., Juhel, J.-B., Vigliola, L., and Meeuwig, J. J. (2015). Low-cost small action cameras in stereo generates accurate underwater measurements of fish. *J. Exp. Mar. Biol. Ecol.* 466, 120–126. doi: 10.1016/j.jembe.2015.02.013

Marshall, A. D., and Bennett, M. B. (2010). Reproductive ecology of the reef manta ray *Manta alfredi* in southern Mozambique. *J. Fish Biol.* 77, 169–190. doi: 10.1111/j.1095-8649.2010.02669.x

Marshall, A. D., Compagno, L. J. V., and Bennett, M. B. (2009). Redescription of the genus Manta with resurrection of *Manta alfredi* (Krefft, 1868) (Chondrichthyes; Myliobatoidei; Mobulidae). *Zootaxa* 2301, 1–28. doi: 10.5281/zenodo.191734

Marshall, A. D., Dudgeon, C. L., and Bennett, M. B. (2011). Size and structure of a photographically identified population of manta rays *Manta alfredi* in southern Mozambique. *Mar. Biol.* 158, 1111–1124. doi: 10.1007/s00227-011-1634-6

Marshall, A. D., Kashiwagi, T., Bennett, M. B., Deakos, M., Stevens, G., McGregor, F., et al. (2018). *Mobula Alfredi (Amended Version of 2011 Assessment)*. London: The IUCN Red List of Threatened Species.

Marshall, A. D., and Pierce, S. J. (2012). The use and abuse of photographic identification in sharks and rays. *J. Fish Biol.* 80, 1361–1379. doi: 10.1111/j.1095-8649.2012.03244.x

McGregor, F., Richardson, A. J., Armstrong, A. J., Armstrong, A. O., and Dudgeon, C. L. (2019). Rapid wound healing in a reef manta ray masks the extent of vessel strike. *PLoS One* 14:e0225681. doi: 10.1371/journal.pone.0225681

Meyer, C. G., Papastamatiou, Y. P., and Holland, K. N. (2010). A multiple instrument approach to quantifying the movement patterns and habitat use of tiger (*Galeocerdo cuvier*) and Galapagos sharks (*Carcharhinus galapagensis*) at French Frigate Shoals, Hawaii. *Mar. Biol.* 157, 1857–1868. doi: 10.1007/s00227-010-1457-x

Minister of Environment EaCC, (2020). *National Parks and Nature Conservancy Act*. New Delhi: Ministry of Environment.

Murray, A., Garrud, E., Ender, I., Lee-Brooks, K., Atkins, R., Lynam, R., et al. (2019). Protecting the million-dollar mantas; creating an evidence-based code of conduct for manta ray tourism interactions. *J. Ecotour.* 19, 132–147. doi: 10.1080/14724049.2019.1659802

Nielsen, A., Bigelow, K. A., Musyl, M. K., and Sibert, J. R. (2006). Improving light-based geolocation by including sea surface temperature. *Fish Oceanogr.* 15, 314–325. doi: 10.1111/j.1365-2419.2005.00401.x

Nielsen, A., and Sibert, J. R. (2007). State–space model for light-based tracking of marine animals. *Can. J. Fish Aquat. Sci.* 64, 1055–1068. doi: 10.1139/f07-064

Notarbartolo di Sciara, G. (1987). A revisionary study of the genus *Mobula rafinesque*, 1810 (Chondrichthyes: Mobulidae) with the description of a new species. *Zool. J. Linn. Soc.* 91, 1–91. doi: 10.1111/j.1096-3642.1987.tb01723.x

O'Malley, M. P., Townsend, K. A., Hilton, P., Heinrichs, S., and Stewart, J. D. (2017). Characterization of the trade in manta and devil ray gill plates in China and South-east Asia through trader surveys. *Aquat. Conserv.* 27, 394–413. doi: 10.1002/aqc.2670

Peel, L. R. (2019). *Movement Patterns and Feeding Ecology of the Reef Manta Ray (Mobula alfredi)*. Ph.D. thesis, University of Western Australia, Perth.

Peel, L. R., Daly, R., Daly, C. A. K., Stevens, G. M. W., Collin, S. P., and Meekan, M. G. (2019a). Stable isotope analyses reveal unique trophic role of reef manta rays (*Mobula alfredi*) at a remote coral reef. *R. Soc. Open Sci.* 6:190599. doi: 10.1098/rsos.190599

Peel, L. R., Stevens, G. M. W., Daly, R., Keating Daly, C. A., Lea, J. S. E., Clarke, C. R., et al. (2019b). Movement and residency patterns of reef manta rays *Mobula alfredi* in the Amirante Islands, Seychelles. *Mar. Ecol. Prog. Ser.* 621, 169–184. doi: 10.3354/meps12995

R Core Team, (2017). *R: A Language and Environment for Statistical Computing*. Vienna: R Foundation for Statistical Computing.

Rohner, C. A., Flam, A. L., Pierce, S. J., and Marshall, A. D. (2017). Steep declines in sightings of manta rays and devil rays (*Mobulidae*) in southern Mozambique. *PeerJ* 5:e3051v3051.

Sequeira, A., Heupel, M., Lea, M. A., Eguíluz, V., Duarte, C., Meekan, M., et al. (2019). The importance of sample size in marine megafauna tagging studies. *Ecol. Appl.* 29:e01947.

Sequeira, A. M. M., Rodríguez, J. P., Eguíluz, V. M., Harcourt, R., Hindell, M., Sims, D. W., et al. (2018). Convergence of marine megafauna movement patterns in coastal and open oceans. *Proc. Natl. Acad. Sci. U.S.A.* 115, 3072–3077. doi: 10.1073/pnas.1716137115

Setyawan, E., Sianipar, A. B., Erdmann, M. V., Fischer, A. M., Haddy, J. A., Beale, C. S., et al. (2018). Site fidelity and movement patterns of reef manta rays (*Mobula alfredi*): mobulidae using passive acoustic telemetry in northern Raja Ampat, Indonesia. *Nat. Conserv. Res.* 3, 1–15. doi: 10.24189/ncr.2018.043

Skomal, G. B., Braun, C. D., Chisholm, J. H., and Thorrold, S. R. (2017). Movements of the white shark *Carcharodon carcharias* in the North Atlantic Ocean. *Mar. Ecol. Prog. Ser.* 580, 1–16. doi: 10.3354/meps12306

Stevens, G. M. W. (2016). *Conservation and Population Ecology of Manta Rays in the Maldives*. PhD thesis, University of York, Heslington.

Stewart, J. D., Jaine, F. R. A., Armstrong, A. J., Armstrong, A. O., Bennett, M. B., Burgess, K. B., et al. (2018). Research priorities to support effective manta and devil ray conservation. *Front. Mar. Sci.* 5:314. doi: 10.3389/fmars.2018.00314

Stoddart, D. R., Coe, M. J., and Fosberg, F. R. (1979). D'Arros and St. Joseph, Amirante Islands. *Atoll. Res. Bull.* 223, 1–48. doi: 10.5479/si.00775630.223.1

Temple, A. J., Kiszka, J. J., Stead, S. M., Wambiji, N., Brito, A., Poonian, C. N. S., et al. (2018). Marine megafauna interactions with small-scale fisheries in the southwestern Indian Ocean: a review of status and challenges for research and management. *Rev. Fish. Biol. Fish.* 28, 89–115. doi: 10.1007/s11160-017-9494-x

Temple, A. J., Wambiji, N., Poonian, C. N. S., Jiddawi, N., Stead, S. M., Kiszka, J. J., et al. (2019). Marine megafauna catch in southwestern Indian Ocean small-scale fisheries from landings data. *Biol. Conserv.* 230, 113–121. doi: 10.1016/j.biocon.2018.12.024

Teo, S. L., Boustany, A., Blackwell, S., Walli, A., Weng, K. C., and Block, B. A. (2004). Validation of geolocation estimates based on light level and sea surface temperature from electronic tags. *Mar. Ecol. Prog. Ser.* 283, 81–98. doi: 10.3354/meps283081

Thums, M., Rossendell, J., Guinea, M., and Ferreira, L. C. (2018). Horizontal and vertical movement behaviour of flatback turtles and spatial overlap with industrial development. *Mar. Ecol. Prog. Ser.* 602, 237–253. doi: 10.3354/meps12650

Venables, S. K., McGregor, F., Brain, L., and van Keulen, M. (2016). Manta ray tourism management, precautionary strategies for a growing industry: a case study from the Ningaloo Marine Park, Western Australia. *Pac. Conserv. Biol.* 22, 295–300.

Vianna, G. M. S., Meekan, M. G., Bornovski, T. H., and Meeuwig, J. J. (2014). Acoustic telemetry validates a citizen science approach for monitoring sharks on coral reefs. *PLoS One* 9:e95565. doi: 10.1371/journal.pone.0095565

Ware, D. (1978). Bioenergetics of pelagic fish: theoretical change in swimming speed and ration with body size. *J. Fish Res. Board Can.* 35, 220–228. doi: 10.1139/f78-036

Webster, C. N., Varpe, Ø, Falk-Petersen, S., Berge, J., Stübner, E., and Brierley, A. S. (2015). Moonlit swimming: vertical distributions of macrozooplankton and nekton during the polar night. *Polar Biol.* 38, 75–85. doi: 10.1007/s00300-013-1422-5

Weng, K. C., Boustany, A. M., Pyle, P., Anderson, S. D., Brown, A., and Block, B. A. (2007). Migration and habitat of white sharks (*Carcharodon carcharias*) in the eastern Pacific Ocean. *Mar. Biol.* 152, 877–894. doi: 10.1007/s00227-007-0739-4

Werry, J. M., Planes, S., Berumen, M. L., Lee, K. A., Braun, C. D., and Clua, E. (2014). Reef-fidelity and migration of tiger sharks, *Galeocerdo cuvier*, across the Coral Sea. *PLoS One* 9:e83249. doi: 10.1371/journal.pone.0083249

Whitcraft, S., O'Malley, M., and Hilton, P. (2014). *The Continuing Threat to Manta and Mobula Rays: 2013-14 Market Surveys, Guangzhou, China*. San Francisco, CA: WildAid.

White, W. T., Corrigan, S., Yang, L., Henderson, A. C., Bazinet, A. L., Swofford, D. L., et al. (2017). Phylogeny of the manta and devilrays (Chondrichthyes: Mobulidae), with an updated taxonomic arrangement for the family. *Zool. J. Linn. Soc.* 182, 50–75. doi: 10.1093/zoolinnean/zlx018

White, W. T., Giles, J., Dharmadi, and Potter, I. C. (2006). Data on the bycatch fishery and reproductive biology of mobulid rays (*Myliobatiformes*) in Indonesia. *Fish. Res.* 82, 65–73. doi: 10.1016/j.fishres.2006.08.008

Zar, J. (1996). *Biostatistical Analysis*. Upper Saddle River, NJ: Prentice-Hall.

Conflict of Interest: The authors declare that the research was conducted in the absence of any commercial or financial relationships that could be construed as a potential conflict of interest.